THE ASTROPHYSICAL JOURNAL, 603:L5–L8, 2004 March 1

THE DISCOVERY OF AN EVOLVING DUST-SCATTERED X-RAY HALO AROUND GRB 031203

S. VAUGHAN,[1] R. WILLINGALE,[1] P. T. O'BRIEN,[1] J. P. OSBORNE,[1] J. N. REEVES,[2,3] A. J. LEVAN,[1] M. G. WATSON,[1] J. A. TEDDS,[1] D. WATSON,[4] M. SANTOS-LLEÓ,[5] P. M. RODRÍGUEZ-PASCUAL,[5] AND N. SCHARTEL[5]

Received 2003 December 23; accepted 2004 January 14; published 2004 February 9

ABSTRACT

We report the first detection of a time-dependent dust-scattered X-ray halo around a gamma-ray burst (GRB). GRB 031203 was observed by *XMM-Newton* starting 6 hr after the burst. The halo appeared as concentric ringlike structures centered on the GRB location. The radii of these structures increased with time as $t^{1/2}$, consistent with small-angle X-ray scattering caused by a large column of dust along the line of sight to a cosmologically distant GRB. The rings are due to dust concentrated in two distinct slabs in the Galaxy located at distances of 880 and 1390 pc, consistent with known Galactic features. The halo brightness implies an initial soft X-ray pulse consistent with the observed GRB.

Subject headings: dust, extinction — Galaxy: structure — gamma rays: bursts — X-rays: general

On-line material: color figures

1. INTRODUCTION

It has long been realized that the small-angle scattering of X-rays by dust grains can result in a detectable X-ray "halo" around a distant X-ray source (Overbeck 1965), with a radial intensity distribution that depends on the dust properties and location. This phenomenon was first detected by Rolf (1983) using data from *Einstein* and confirmed by later observations (e.g., Mauche & Gorenstein 1986; Predehl et al. 1991).

In the case of gamma-ray bursts (GRBs), the transient nature of the burst combined with the large initial X-ray flux means that X-ray scattering may be visible for a short period of time with a relatively high surface brightness. As the transient flux passes through a dust slab between the observer and the GRB, the scattering process introduces a time delay in which the X-rays at larger angles to the line of sight arrive increasingly delayed with respect to the nonscattered X-rays. Thus, the dust allows us to view the GRB X-ray flux at earlier times. The time-dependent X-ray halo around the GRB can, in principle, be used to provide detailed information on the location, spatial distribution, and properties of the dust and the distance to and brightness of the GRB (e.g., Trümper & Schöfelder 1973; Klose 1994; Miralda-Escudé 1999; Draine 2003). Images of transient X-ray sources seen in scattered light are analogous to "light echos" seen around some supernovae (e.g., SN 1987A; Xu, Crotts, & Kunkel 1995).

Scattered X-rays observed at an angle θ from the line of sight to a GRB arrive after the direct emission with a time delay τ_s given by

$$\tau_s = \frac{(1 + z_s) D_s D_g \theta^2}{2 c D_{g,s}}, \quad (1)$$

where z_s and D_s are the redshift and angular diameter distance of the scattering dust, D_g is the angular diameter distance of the GRB, and $D_{g,s}$ is the angular diameter distance from the dust to the GRB (Miralda-Escudé 1999).

Here we discuss the case of GRB 031203 observed by *XMM-Newton* on two occasions shortly after the burst. The first observation revealed the first dust-scattered X-ray halo detected around a GRB.

2. OBSERVATIONS AND DATA ANALYSIS

GRB 031203 was detected by the Imager on Board the *INTEGRAL* Satellite on 2003 December 3 at 22:01:28 UT as a single peaked burst with a duration of 30 s and peak flux of 1.3×10^{-7} ergs s^{-1} cm^{-2} in the 20–200 keV band (Gotz et al. 2003; Mereghetti & Gotz 2003). A 58 ks *XMM-Newton* observation of the field began at 2003 December 4, 04:09:29 UT. Several X-ray sources were detected within the 2.′5 radius *INTEGRAL* error circle (Santos-Lleó & Calderón 2003), the brightest of which (S1) appeared to fade through the observation (Rodríguez-Pascual et al. 2003) and was interpreted as the X-ray afterglow of GRB 031203. We refined the astrometric position of the afterglow by performing a cross-correlation with the USNO-A2.0 catalog; the improved S1 position was R.A. = $08^h02^m30\overset{s}{.}19$, decl. = $-39°51'04\overset{''}{.}0$ (J2000.0; 1 σ error $0\overset{''}{.}7$; Tedds et al. 2003).

The position in the Galactic plane ($l = 255°$, $b = -4.6°$) results in high optical extinction [$E(B-V) = 1.0$; Schlegel, Finkbeiner, & Davis 1998]. Optical/IR observations failed to locate an afterglow. Radio observations did locate a transient source location consistent with the X-ray afterglow (Soderberg, Kulkarni, & Frail 2003), and optical imaging and spectroscopy revealed a candidate host galaxy at $z = 0.105$ that shows star-forming features typical of GRB hosts (Prochaska et al. 2003a, 2003b). Our refined location for the X-ray afterglow is within $0\overset{''}{.}5$ of the optical galaxy and consistent with the position of the radio source.

[1] Department of Physics and Astronomy, University of Leicester, University Road, Leicester LE1 7RH, UK; sav2@star.le.ac.uk, rw@star.le.ac.uk, pto@star.le.ac.uk, julo@star.le.ac.uk, anl@star.le.ac.uk, mgw@star.le.ac.uk, jat@star.le.ac.uk.

[2] Laboratory for High Energy Astrophysics, Code 662, NASA Goddard Space Flight Center, Greenbelt Road, Greenbelt, MD 20771; jnr@milkyway.gsfc.nasa.gov.

[3] Universities Space Research Association.

[4] Niels Bohr Institute for Astronomy, Physics and Geophysics, University of Copenhagen, Julian-Maries Vej 30, DK-2100 Copenhagen Ø, Denmark; darach@astro.ku.dk.

[5] *XMM-Newton* SOC, Villafranca, Apartado 50727, E-28080 Madrid, Spain; msantos@xmm.vilspa.esa.es, prodrigu@xmm.vilspa.esa.es, norbert.schartel@esa.int.

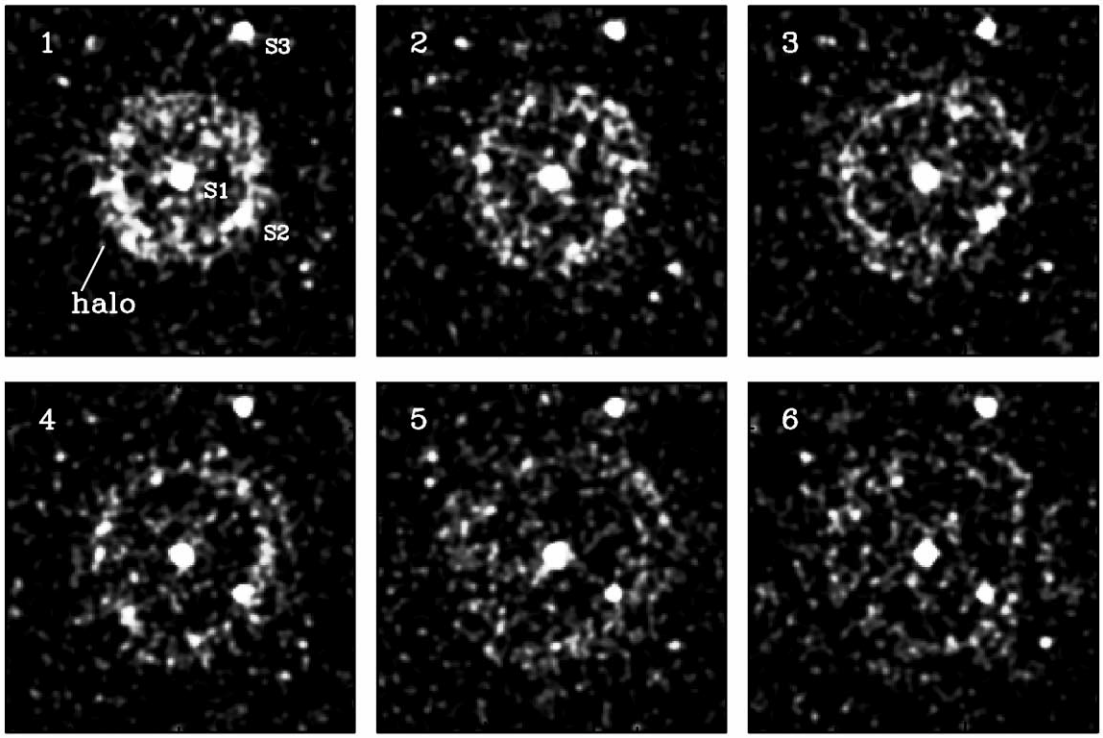

FIG. 1.—Combined MOS images of GRB 031203 covering the 0.7–2.5 keV range, spanning 10′ on a side. The data were divided into 10 contiguous time intervals lasting 5780 s. The images obtained from the first six time slices are shown (smoothed using a 6″ Gaussian kernel). The three brightest point sources (S1, S2, and S3) are marked. [*See the electronic edition of the Journal for a color version of this figure.*]

During the first *XMM-Newton* observation the GRB was observed on axis with all European Photon Imaging Camera (EPIC) instruments in full-frame modes (Strüder et al. 2001; Turner et al. 2001). A second 54 ks *XMM-Newton* observation was obtained on 2003 December 6 in which the GRB was ≈6′ off axis. The observational details and the GRB spectrum and light curve are discussed in detail in Watson et al. (2004).

The extraction of science products followed standard procedures using the *XMM-Newton* Science Analysis System (SAS ver. 5.4.1). The EPIC data were processed using the SAS chains to produce calibrated event lists and remove background flares. GRB afterglow source counts were extracted from circular regions (radius 34″), and background counts were estimated from a large off-axis region free from obvious point sources and the halo. The GRB afterglow fades as $(t - t_0)^{-0.4}$, where t_0 is the time of the GRB, which is unusually slow for GRB X-ray afterglows.

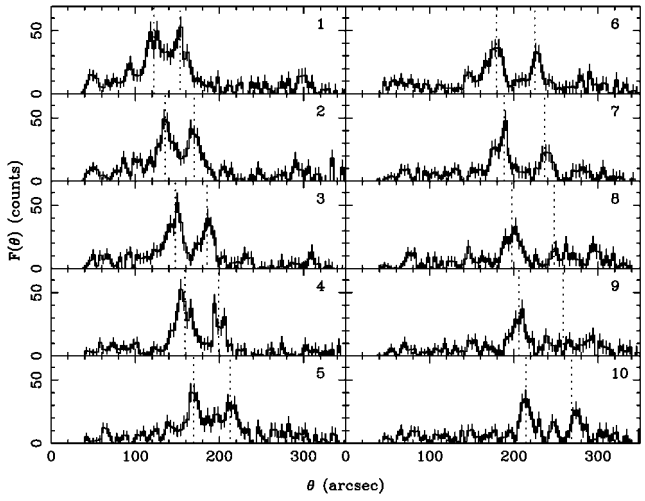

FIG. 2.—Radial profile of counts about the GRB 031203 afterglow from 10 contiguous time intervals (derived from the combined MOS 0.7–2.5 keV images). The afterglow itself (S1) and the next two brightest point sources (S2 and S3) were removed prior to calculating the profiles. The two peaks corresponding to the two expanding rings are obvious. The dotted lines denote the best-fitting $\theta \propto (t - t_0)^{1/2}$ functions (see Fig. 3).

3. THE X-RAY HALO

The X-ray image from the first *XMM-Newton* observation reveals an extended circular halo concentric with the GRB 031203 afterglow (see Fig. 1). This halo was seen in all three cameras of the EPIC instrument, is unique to this observation, and is not due to scattered optical or X-ray light within the instrument. Summing the entire observation, the halo had the form of a virtually complete ring (Vaughan et al. 2003), but splitting the observation into contiguous time intervals revealed distinct rings that increased in radius through the observation.

In order to better quantify this expansion, EPIC MOS images were produced for 10 contiguous time intervals of 5780 s duration, spanning the entire first observation and binned to 4″ pixels. We concentrate on the MOS data as the halo lies over several chip gaps in the EPIC pn images, but the same halo was seen in both. The radial profiles of the images about the afterglow were calculated removing the three brightest point sources within the region of interest (S1, S2, and S3 in Fig. 1) by ignoring all counts within 40″ from the centroid of each source. The radial profiles were then background subtracted using the mean level from the 350″–400″ annulus, which is well outside the detected halo. The resulting count profiles as a function of radius are shown in Figure 2. The strongest peak moved outward from ~120″ to ~220″ during the observation, while a second peak moved from ~160″ to ~270″.

The radial positions of the two rings were measured from

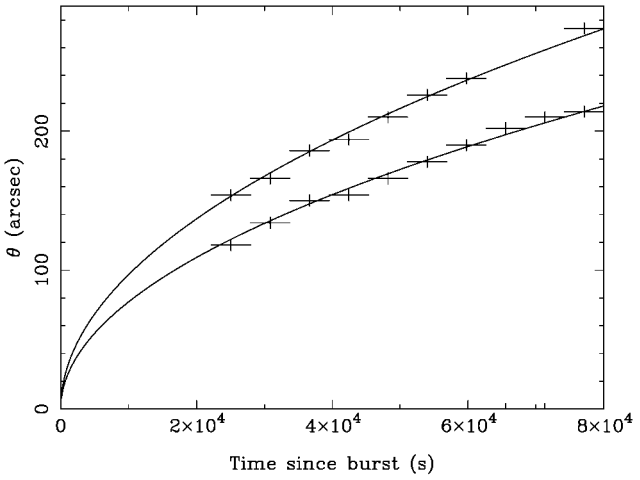

FIG. 3.—Expansion of the two rings around GRB 031203 with time. The radius of each ring was measured from the local maxima of the radial profiles (Fig. 2). In both cases the expansion was well fitted with a functional form $\theta \propto (t - t_0)^{1/2}$. The errors were assumed to be the width of the bin size used for the radial profile measurement.

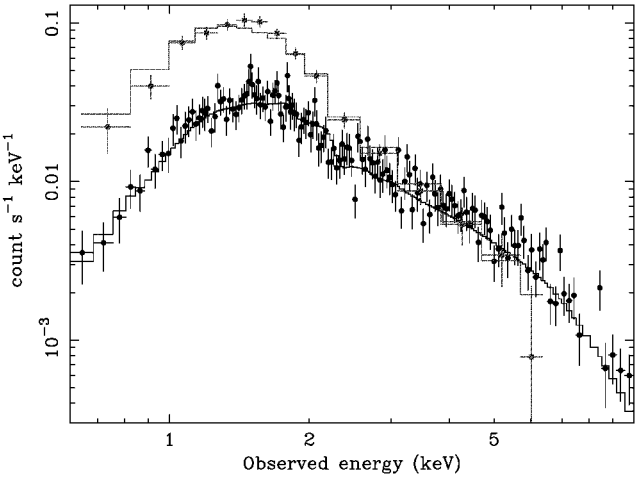

FIG. 4.—Absorbed power-law model fits to the EPIC pn spectra of the GRB 031203 afterglow (*circles, thick line*) integrated over the entire observation and the dust halo (*squares, thin line*) integrated over the first half (27895 s) of the observation (during which the surface brightness was high enough for a reasonable spectral extraction). This clearly demonstrates that the spectrum of the halo is significantly steeper than the afterglow. [*See the electronic edition of the Journal for a color version of this figure.*]

the local maxima of the two peaks in the radial distributions. Figure 3 shows the change in radii as a function of time, and both were well fitted by a simple power law [$\theta \propto (t - t_0)^{\alpha}$]. Fixing $t_0 = 0$, the indices of the power-law expansions were measured to be $\alpha = 0.53 \pm 0.04$ and 0.51 ± 0.05 for the inner and outer rings, respectively (errors are 90% confidence intervals), consistent with the $\theta \propto (t - t_0)^{1/2}$ expansion predicted for a scattered halo. As a consistency check we allowed t_0 to be a free parameter but fixed $\alpha = 0.5$ and refitted to derive limits of $t_0 = 2794^{+2765}_{-3178}$ and 2005^{+2512}_{-2867} s for the inner and outer ring, respectively, both consistent with $t_0 = 0$. The second *XMM-Newton* observation obtained 3 days after the burst showed no evidence of any ringed structure.

The distance to the GRB is large (adopting the redshift of the putative host galaxy), the time delay is short, and θ is relatively large, thus to a good approximation $D_g = D_{g,s}$ and $(1 + z_s) = 1$ in equation (1), hence $D_s = 2c\tau_s/\theta^2$. Assuming $\theta \propto (t - t_0)^{1/2}$ and $t_0 = 0$, the data in Figure 3 imply that the scattering dust slabs are located at distances from the observer of $D_1 = 1388 \pm 32$ pc and $D_2 = 882 \pm 20$ pc, corresponding to the inner and outer ring, respectively. At these distances, the ring diameters probe size scales of 2–3 pc in the dust-scattering medium.

The halo spectrum was extracted from an annulus with radii 110″–220″ using only the first half of the observation; the decreased surface brightness of the halo at later times makes spectral extraction unreliable. A background spectrum was extracted from a large off-axis region (avoiding the halo and other point sources). Figure 4 shows the halo spectrum compared to the afterglow spectrum. The spectrum of the halo is much steeper than that of the afterglow. Fitting with a simple absorbed power law yielded photon indices of $\Gamma = 1.98 \pm 0.05$ and 3.03 ± 0.14 for the afterglow and halo, respectively. The best-fitting absorbing column was $N_{\rm H} = 8.8 \pm 0.5 \times 10^{21}$ cm^{-2} when fixed to be the same for both afterglow and halo spectra. This is larger than the Galactic value of $N_{\rm H} = 6.1 \times 10^{21}$ cm^{-2} (Dickey & Lockman 1990). The specific fluxes at $t = 36650$ s after the burst at 1 keV are $1.5^{+0.2}_{-0.1} \times 10^{-4}$ photons cm^{-2} s^{-1} keV^{-1} for the afterglow and $6.0 \pm 0.4 \times 10^{-4}$ photons cm^{-2} s^{-1} keV^{-1} for the halo.

To model the dust-scattering medium, we have simultaneously fitted the 10 radial profiles shown in Figure 2 using the differential and total scattering cross sections of the Rayleigh-Gans approximation (Mauche & Gorenstein 1986). This is a valid approximation if the grain radius in units of μm is much less than the X-ray photon energy in units of keV (Smith & Dwek 1998). We assume that the dust is confined to two slabs at distances D_1 and D_2 with thickness ΔD. The halo seen is created by the combination of the soft X-ray pulse from the GRB and the subsequent afterglow. The observed angular width of the rings results from a combination of the duration of the soft X-ray pulse, Δt, ΔD, and the point-spread function (PSF) of the telescope. The width of the PSF corresponds to $\Delta t \sim 1000$ s or $\Delta D \sim 100$ pc. Given that the GRB is very short, ~30 s (Mereghetti & Gotz 2003), we assume that $\Delta t \ll 1000$ s, and hence, allowing for the PSF, the observed broadening of the rings, 20″, gives us an estimate of the slab thickness, $\Delta D = 130 \pm 50$ pc.

The angular and temporal distribution was well fitted using grains with radii in the range $0.15\ \mu{\rm m} < a < 0.25\ \mu{\rm m}$. Smaller grains scatter to much larger angles (not visible because the time elapsed since the burst is too small), and the upper limit to the grain size distribution is expected to be $\approx 0.3\ \mu$m (Predehl et al. 1991). Using this range of grain sizes, we require the initial GRB pulse and afterglow to have a photon index of $\Gamma \sim 2.0$ (as observed for the afterglow from 6 hr) to match the observed photon index of the halo ($\Gamma = 3.0$).

The brightness of the halo depends on the product of the differential scattering cross sections of the grains, the column densities of the grains in the slabs, and the integrated flux of the X-ray pulse and afterglow. Interstellar extinction maps show structure in the GRB direction, with a considerable increase to $A_V \approx 2$ mag at a distance of ~1.3 kpc (Neckel & Klare 1980). This distance is consistent with the location of the more distant dust slab that we detect. Adopting a mean grain size of $a = 0.2\ \mu$m, an $A_V = 2$ mag corresponds to a grain column density of 1.5×10^8 cm^{-2} (Mauche & Gorenstein 1986). The best fit to the ring structure (χ^2/degrees of freedom = 836/489) results from dividing this column density between the two slabs, $N_1 \sim 1 \times 10^8$ and $N_2 \sim 0.5 \times 10^8$ cm^{-2} (i.e., most of the dust is in the more distant slab). Using these values and $a = 0.20 \pm 0.05$, the time-integrated flux required for the soft X-ray pulse is 1600 ± 800 photons cm^{-2} keV^{-1} at 1 keV. As-

suming a 30 s rectangular pulse, this is equivalent to ~5 crabs; using $\Gamma = 2$ the predicted GRB flux in the 20–200 keV band is 2.4 ± 1.2 photons cm^{-2} s^{-1}. Given the assumptions (e.g., spectral shape), this is in reasonable agreement with the value reported for GRB 031203 (peak of ~1.2 photons cm^{-2} s^{-1}; Gotz et al. 2003; Mereghetti & Gotz 2003). The X-ray burst is very bright compared to the afterglow (see Watson et al. 2004). Extrapolating the decay of the afterglow (§ 2) to the time of the GRB accounts for only ~2% of the halo emission.

The line of sight to GRB 031203 passes close to the center of the Gum Nebula that appears as a 28° diameter sphere in Hα centered at $l = 258°$, $b = -2°$ (Chanot & Sivan 1983). The Gum Nebula is likely to be a supershell created by repeated supernovae explosions within it. Reynoso & Dubner (1997) detected a neutral gas disk (H I) associated with the Gum Nebula, located ~500 ± 100 pc from us, with a radius of ~150 pc. The dust slab nearest to us may be associated with the rear face of the Gum Nebula that is known to have a concentration of molecular clouds (Woermann, Gaylard, & Otrupcek 2001).

This Letter is based on observations obtained with *XMM-Newton*, an ESA science mission with instruments and contributions directly funded by ESA Member States and the US (NASA). S. V. and A. J. L. acknowledge support from PPARC, UK. We acknowledge the benefits of collaboration within the Research and Training Network "Gamma-Ray Bursts: An Enigma and a Tool," funded by the European Union under contract HPRN-CT-2002-00294. We thank the anonymous referee for a constructive report.

REFERENCES

Chanot, A., & Sivan, J. P. 1983, A&A, 121, 19
Dickey, J. M., & Lockman, F. J. 1990, ARA&A, 28, 215
Draine, B. T. 2003, ApJ, 598, 1026
Gotz, D., Mereghetti, S., Beck, M., Borkowski, J., & Mowlavi, N. 2003, GCN Circ. 2459 (http://gcn.gsfc.nasa.gov/gcn/gcn3/2459.gcn3)
Klose, S. 1994, A&A, 289, L1
Mauche, C. W., & Gorenstein, P. 1986, ApJ, 302, 371
Mereghetti, S., & Gotz, D. 2003, GCN Circ. 2460 (http://gcn.gsfc.nasa.gov/gcn/gcn3/2460.gcn3)
Miralda-Escudé, J. 1999, ApJ, 512, 21
Neckel, Th., & Klare, G. 1980, A&AS, 42, 251
Overbeck, J. W. 1965, ApJ, 141, 864
Predehl, P., Bräuniger, H., Burket, W., & Schmitt, J. H. M. M. 1991, A&A, 246, L40
Prochaska, J., Bloom, J. S., Chen, H. W., Hurley, K., Dressler, A., & Osip, D. 2003a, GCN Circ. 2482 (http://gcn.gsfc.nasa.gov/gcn/gcn3/2482.gcn3)
Prochaska, J., Chen, H. W., Hurley, K., Bloom, J. S., Graham, J. R., & Vacca, W. D. 2003b, GCN Circ. 2475 (http://gcn.gsfc.nasa.gov/gcn/gcn3/2475.gcn3)
Reynoso, E. M., & Dubner, G. M. 1997, A&AS, 123, 31
Rodríguez-Pascual, P., Santos-Lleó, M., Gonzales-Riestra, R., Schartel, N., & Altieri, B. 2003, GCN Circ. 2474 (http://gcn.gsfc.nasa.gov/gcn/gcn3/2474.gcn3)
Rolf, D. P. 1983, Nature, 302, 46
Santos-Lleó, M., & Calderon, P. 2003, GCN Circ. 2464 (http://gcn.gsfc.nasa.gov/gcn/gcn3/2464.gcn3)
Schlegel, D. J., Finkbeiner, D. P., & Davis, M. 1998, ApJ, 500, 525
Smith, R. K., & Dwek, E. 1998, ApJ, 503, 831
Soderberg, A. M., Kulkarni, S. R., & Frail, D. A. 2003, GCN Circ. 2483 (http://gcn.gsfc.nasa.gov/gcn/gcn3/2483.gcn3)
Strüder, L., et al. 2001, A&A, 365, L18
Tedds, J., et al. 2003, GCN Circ. 2490 (http://gcn.gsfc.nasa.gov/gcn/gcn3/2490.gcn3)
Trümper, J., & Schönfelder, V. 1973, A&A, 25, 445
Turner, M. J. L., et al. 2001, A&A, 365, L27
Vaughan, S., et al. 2003, GCN Circ. 2489 (http://gcn.gsfc.nasa.gov/gcn/gcn3/2489.gcn3)
Watson, D., et al. 2004, ApJ, submitted (astro-ph/0401225)
Woermann, B., Gaylard, M. J., & Otrupcek, R. 2001, MNRAS, 325, 1213
Xu, J., Crotts, A. P. S., & Kunkel, W. E. 1995, ApJ, 451, 806